Secure medical image watermarking based on reversible data hiding with Arnold's cat map

Aulia Arham [a,1,*], Novia Lestari [a,2]

[a] Department of Information System, State Islamic University Imam Bonjol, Padang 25171, Indonesia
[1] auliaarham@uinib.ac.id; [2] noviia.lestari@uinib.ac.id
* corresponding author

ARTICLE INFO

Article history
Received February 16, 2023
Revised April 14, 2023
Accepted May 21, 2023
Available online October 15, 2023

Keywords
Medical image
Reversible data hiding
Difference expansion
Chaotic map
Arnold's cat map

ABSTRACT

The process of restoring medical images to their original form after the extraction process in application watermarking is crucial for ensuring their authenticity. Inaccurate diagnoses can occur due to distortions in medical images from conventional data embedding applications. To address this issue, reversible data hiding (RDH) method has been proposed by several researchers in recent years to embed data in medical images. After the extraction process, images can be restored to their original form with a reversible data-hiding method. In the past few years, several RDH methods have been rapidly developed, which are based on the concept of difference expansion (DE). However, it is crucial to pay attention to the security of the medical image watermarking method, the embedded data with RDH method can be easily modified, accessed, and altered by unauthorized individuals if they know the employed method. This research suggests a new approach to secure the RDH method through the use of Chaotic Map-based Arnold's Cat Map algorithms on the medical images. Data embedding was performed on random medical images using a DE method. Four gray-scale medical image modalities were used to assess the proposed method's efficacy. In our approach, we can incorporate capacity up to 0.62 bpp while maintaining a visual quality up to 41.02 dB according to PSNR and 0.9900 according to SSIM. The results indicated that it can enhance the security of the RDH method while retaining the ability to embed data and preserving the visual appearance of the medical images.

1. Introduction

Medical images are visual representations of the functions of some of a patient's organs or tissues that are used for diagnosis or disease detection. These images can be obtained through methods such as Computerized Radiography, CT scans, Ultrasound, MRI, and X-rays [1]. The advancements in internet technology have made it simpler for people to access digital images. Image processing software can be used to manipulate, harm, or distribute digital data. The ease of image manipulation highlights the importance of image authentication in applications where verifying the image's integrity and authenticity is critical, such as in medical, military, and forensic imaging [2]. Recently, various authentication methods have been suggested to ensure the authenticity of image content, which involves embedding data within the image. However, Traditional methods of embedding data, such as LSB or using techniques such as Discrete Cosine Transform, Discrete Wavelet Transform, or Discrete Fourier Transform to embed data into the frequency domain [3] leads to permanent distortion in the image, as in research [4]–[12]. Traditional watermarking techniques applied to medical images can result in permanent distortion, leading to misdiagnosis. The security of medical images is a pressing concern,

particularly in ensuring the integrity of images when they and patients' information are transmitted over the internet [5], [6].

Reversible Data Hiding (RDH) methods have received significant attention in research in the past few years due to its capability to restore the original image in a reversible manner. [4], [13]–[17]. An example of simple RDH method is the Difference Expansion (DE), Tian [18] was the first to introduce this method. The method involved embedding data bits into the difference of pixel pairs. The difference of the pixel pair is divided into 8-bit planes, and the bits of data are embedded in the last bit. Using this method leads to an even greater expansion in the difference value between pairs of pixel. Over the past few years, several RDH methods have been rapidly developed, which are based on the concept of DE method. In 2017, Arham *et al.* [2] improved the DE method by using block of pixel with each block containing four pixels. To embedding data, one of the pixel is used as the reference point, the algorithm calculates the differences between pixel pairs, resulting in three distinct values that can be utilized for embedding data. This method utilizes IRDE (Improved Reversible Data Embedding) to reduce the differences between pixels in the DE method prior to performing the data embedding process. The results show this method has a higher embedding capacity and produces images with superior visual quality. Other RDH based on DE approaches were presented in [1], [4], [16], [17], [19]–[29]. However, security remains an issue in these RDH methods as the embedded data can be easily accessed and altered by unauthorized individuals if they know the employed method.

To increase the security of the RDH methods, several researchers have proposed various methods. In the year 2021, Wu *et al.* [30] introduced a new RRBE technique that utilizes adaptive prediction-error labeling (APL) to embed encrypted data into encrypted images at specific locations, resulting in a marked encrypted image. Meenpal *et al.* [31] introduced a secure RDH method in the year 2022, where data is embedded into low-frequency blocks of an image using the DE method within the Integer Wavelet Transform (IWT) domain. In other researchers were presented in [32]–[35] proposed secure RDH with the data encrypted are embedded into the image with Histogram Shifting method. The previously proposed method typically involved encrypting the embedded confidential data to increase the security of the RDH approach.

The objective of this research is to enhance the security of the DE-based RDH method in medical images. The suggested method combines the RDH method presented by Arham *et al.* [2] with the chaotic logistic map technique, utilizing the Arnold's Cat Map algorithm. In 2021, Sahu [36] proposed a method for secure data hiding used a logistic map. However, these techniques alter the LSB of the original image and are considered secure, but they cause permanent distortion to the image and cannot be reversed, making them unsuitable for applications where image preservation is crucial, such as medical imaging.

The paper's structure comprises four sections. Section I presents the research background and a summary of prior research related to the suggested methods. Section II presents a comprehensive description of the proposed technique, while Section III demonstrates the outcomes of the experiments. Lastly, Section IV provides the conclusion.

2. Method

This section describes the supportive methods for the proposed method, including DE, IRDE, Multiple-layer data hiding, Arnold's Cat Map, and the proposed method.

2.1. Difference Expansion (DE)

The DE technique was initially introduced by Tian [10]. This method involves embedding data in a grayscale image by utilizing the difference of the pixel pair, while keeping their average value intact. On two pairs of neighboring pixels is divided into 8-bit planes are P_1 and P_2 then the difference between them v, and the average is $\bar{x}$, of the pair of pixels can be represented as Equation (1).

$$\overline{x} = \frac{p_1 + p_2}{2},\ v = p_1 - p_2 \tag{1}$$

The embedding procedure involves expanding the difference pixel v. The process of embedding the data bit b involves expanding it based on Equation (2). The difference pixel v that now contains data is used to create a new pixel. The creation is performed using the unchanging average pixel, as stated in Equation (3).

$$v' = 2 \times v + s \tag{2}$$

$$p'_1 = \overline{x} + \frac{v'+1}{2},\ p'_2 = \overline{x} - \left\lfloor \frac{v'}{2} \right\rfloor \tag{3}$$

The new pixels P'_1 and P'_2, must not exceed the maximum (255) or fall below the minimum (0) values for grayscale pixels. To ensure this, the difference pixels containing the data must meet the conditions specified in Equation (4).

$$\begin{cases} |v'| \le 2 \times (255 - \overline{x}), if\ 128 \le \overline{x} \le 255 \\ |v'| \le 2 \times \overline{x} + 1, if\ 0 \le \overline{x} \le 127 \end{cases} \tag{4}$$

2.2. DE of Quad

The method of DE serves as the foundation for the Quad Difference Expansion. This approach splits the image into 2×2 blocks, each containing 4 pixels, and transforms these blocks into vectors $p = (p_0, p_1, p_2, p_3)$, as shown in Fig. 1. To embedding data, one of the pixels is used as the reference point, the algorithm calculates the differences between pixel pairs using Equation (5), resulting in three distinct values that can be utilized for embedding data, resulting in the vector $v = (v_1, v_2, v_3)$. The original image can be restored using Equation (6), which is the inverse of Equation (5).

$$\begin{cases} v_1 = p_1 - p_0 \\ v_2 = p_2 - p_1 \\ v_3 = p_3 - p_2 \end{cases} \tag{5}$$

$$\begin{aligned} p_0 &= v_0 - \left\lfloor \frac{3v_1 + 2v_2 + v_3}{4} \right\rfloor \\ p_1 &= v_1 + p_0 \\ p_2 &= v_2 + p_1 \\ p_3 &= v_3 + p_2 \end{aligned} \tag{6}$$

Data embedding can be done through Equation (7) and Equation (8). If a block is classified as expandable, data is embedded using Equation (7). If a block is labeled as changeable (in cases of overflow or underflow), data embedding uses Equation (8). Blocks categorized as unchangeable do not have data embedded in them.

$$\begin{cases} v'_1 = 2 \times v_1 + s_1 \\ v'_2 = 2 \times v_2 + s_2 \\ v'_3 = 2 \times v_3 + s_3 \end{cases} \tag{7}$$

$$\begin{cases} v'_1 = 2 \times \frac{v_1}{2} + s_1 \\ v'_2 = 2 \times \frac{v_2}{2} + s_2 \\ v'_3 = 2 \times \frac{v_3}{2} + s_3 \end{cases} \tag{8}$$

The value of the differences between the pixels that have had data embedded must meet the requirements outlined in Equation (9) to prevent underflow and overflow. Once the data embedding process has finished, the new pixels p'_i can be formed using Equation (10). This method has a theoretical maximum capacity for data embedding of 0.75 bits per pixel.

$$\begin{cases} 0 \le v_0 - \left\lfloor \frac{v_1+v_2+v_3}{4} \right\rfloor \le 255 \\ 0 \le v_1' + p_0 \le 255 \\ 0 \le v_2' + p_1 \le 255 \\ 0 \le v_3' + p_2 \le 255 \end{cases} \quad (9)$$

$$\begin{aligned} p_0 &= p_0 \\ p_1 &= v_1' + p_0 \\ p_2 &= v_2' + p_1 \\ p_3 &= v_3' + p_2 \end{aligned} \quad (10)$$

2.3. Improved Reduced DE (IRDE)

The IRDE method was utilized to decrease the pixel differences in the DE method before the data embedding procedure takes place. Yi made changes to RDE by executing the reduction process according to Equation (11). The location map is then produced based on Equation (12).

$$v_i' = \begin{cases} v_i - 2^{\log_2|v_i|-1}, if\ 2 \times 2^{n-1} \le v_i \le 3 \times 2^{n-1} - 1 \\ v_i - 2^{\log_2|v_i|}, \quad if\ 3 \times 2^{n-1} \le v_i \le 4 \times 2^{n-1} - 1 \end{cases} \quad (11)$$

$$n = \lfloor \log_2|v_i| \rfloor \quad (12)$$

$$LM = \begin{cases} 0, & if\ 2 \times 2^{n-1} \le v_i \le 3 \times 2^{n-1} - 1 \\ 1, & if\ 3 \times 2^{n-1} \le v_i \le 4 \times 2^{n-1} - 1 \end{cases} \quad (13)$$

The extraction process utilizes the location map for revealing hidden data and returning the image to its original appearance. Results from experiments conducted by Yi indicate that IRDE has a greater data capability to embed and improved visual quality compared to RDE.

$$v_i = \begin{cases} v_i' + 2^{\log_2|v_i'|+1}, & if\ LM = 1 \\ v_i' + 2^{\log_2|v_i'|}, & if\ LM = 0 \end{cases} \quad (14)$$

2.4. Multiple-layer embedding

In 2017, Arham *et al.* [2] introduced a RDH method that employed layered data embedding. This method combined the DE fo Quad method and the IRDE method. The IRDE method was used to decrease the difference among pixel pairs in Quad's DE, thereby enhancing the image's capacity for incorporation and visual quality after embedding. In this method, each block $p = (p_0, p_1, p_2, p_3)$ is transformed into a vector $v = (v_1, v_2, v_3)$ by using Equation (5). This refers to calculating the difference between the pixels in vector u and designating p_0 as the reference point.

2.5. Arnold's Cat Map

Over the past few years, The field of information security has extensively employed chaos theory, including watermarking and cryptography. Its extreme sensitivity to the initial value of the chaos algorithm makes it ideal for use in information security, especially watermarking and cryptography. Arnold's Cat Map is one such chaotic function that is both invertible and reversible. It was first introduced by Vladimir Arnold'sin 1960, with the word "cat" used because a picture of a cat was used in his experiments. Arnold's Cat Map produces new coordinates (x', y') that are the result of transforming the existing coordinates (x, y) in an $N\ x\ N$ image. The iteration used is Equation (15).

$$\begin{bmatrix} x_{i+1} \\ y_{i+1} \end{bmatrix} = \begin{bmatrix} 1 & b \\ c & bc+1 \end{bmatrix} \begin{bmatrix} x_i \\ y_i \end{bmatrix} mod\ (N) \quad (15)$$

The coordinates (x_i, y_i) refer to the location of the pixels in the image (x_{i+1}, y_{i+1}) which change position after i iteration. b and c are positive integers. In order for the transformation to stay within the same image area, the determinant of the matrix $\begin{bmatrix} 1 & b \\ c & bc+1 \end{bmatrix}$ must equal 1, meaning it is area-preserving. Arnold's Cat Map transforms each pixel to a unique new pixel position, so its mapping is

one-to-one. The Arnold's Cat Map iteration is repeated m times and produces a random image each time. b, c and m, the number of rounds in Arnold's Cat Map can serve as a secret key. The process of Arnold's Cat Map involves shifting the image in the y direction, followed by shifting in the x direction, during each iteration. However, the result may fall outside the image area, so all results are taken modulo N to ensure they stay within the image area (area preserving).

$$\begin{bmatrix} x_i \\ y_i \end{bmatrix} = \begin{bmatrix} 1 & b \\ c & bc+1 \end{bmatrix} \begin{bmatrix} x_{i+1} \\ y_{i+1} \end{bmatrix} mod\ (N) \tag{16}$$

The Arnold's Cat Map is iterated m times, and there is a value of T such that after T iterations, the image will return to its original form. This means that the ACM is reversible and has a period of T. Researchers have found that T is less than $3N$. The iteration process on the 'sailboat' image is shown in Fig. 1, and it becomes more random with each iteration. By the 96th iteration, the 'sailboat' image returns to its original form, so its period is $T = 96$. The ACM, like other deterministic chaos functions, can be reconstructed using the same key (b, c and m) into the original image. The decryption process is finished because the final iteration result is identical to the original image.

2.6. The proposed Method

The proposed method aims to enhance the security of the method introduced by Arham *et al.* [2] by applying Arnold's Cat Map to scramble the picture on the cover prior to the embedding procedure.

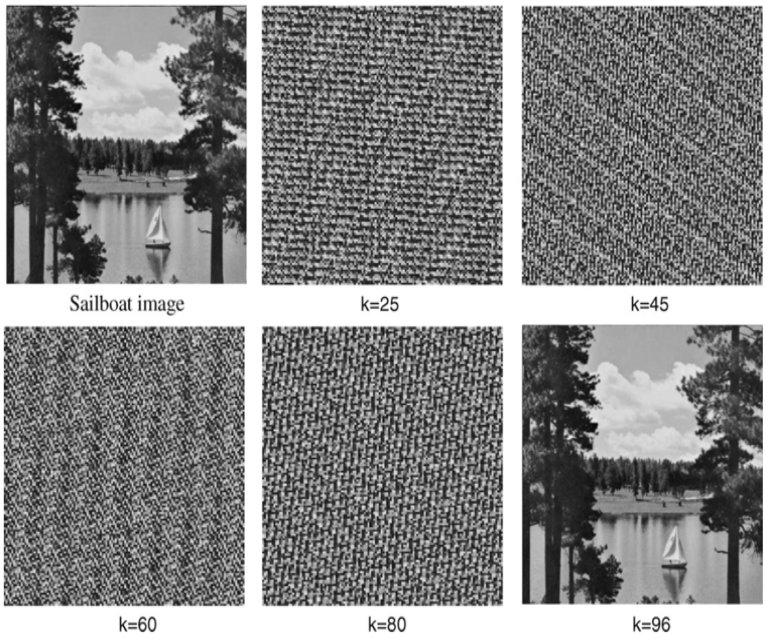

Fig. 1. The process of Iteration in Arnold's Cat Map on the "sailboat" image, with a period $T = 96$.

2.6.1. Embedding Procedure

The steps or process outlined for embedding (Fig. 2) start with applying the Chaos Arnold's Cat Map function to image I for a specific number of iterations (k-times), the resulting scrambled image is (I_{src}). Then, without any overlapping, the scrambled image I_{src} is separated into blocks, with each block containing four pixels. Each block is transformed into a vector $p = (p_0, p_1, p_2, p_3)$. The differences between each vector u are calculated to produce another vector (v_1, v_2, v_3).

The differences in the values of vector v are then reduced using the IRDE method to form vector Q. Where, Vector Q is divided into three categories: S_1, S_2, and S_3. S_1 contains all expandable blocks with $Q_1 \leq T_1, Q_2 \leq T_2$, and $Q_3 \leq T_3$, where T_1, T_2, and T_3 are predetermined thresholds. S_2 contains all changeable blocks not in S_1, and S_3 contains all unchangeable blocks. S_3 will also return the original values of S_2 and S_3 from before the reduction process.

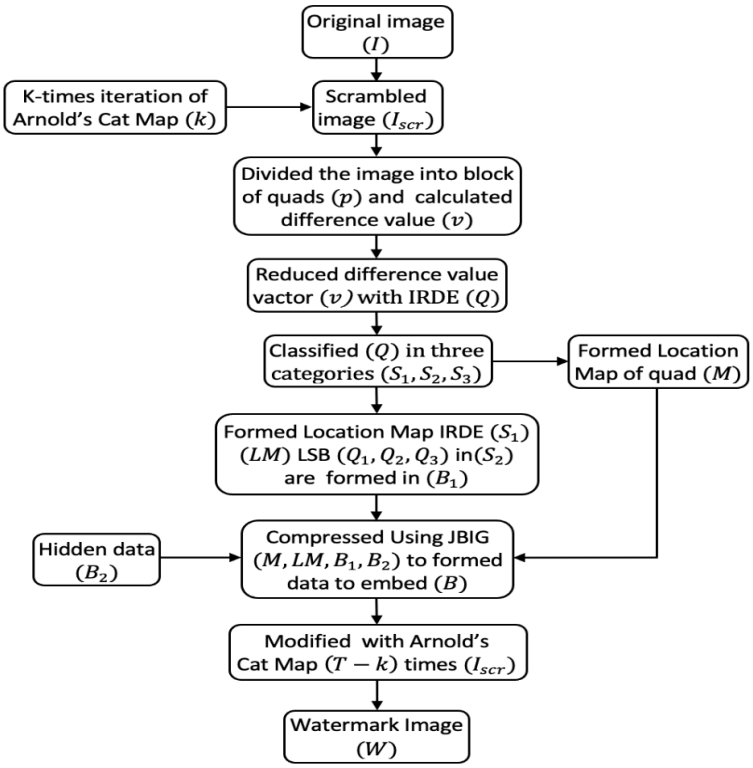

Fig. 2. Embedding procedure of proposed method

A location map M is formed to identify the location of blocks, with 1 indicating the location of S_1 and 0 indicating the location of S_2. After applying the IRDE method to reduce the size of certain blocks, a reduced location map LM is created to keep track of their blocks reduced. Then, the LSB of the Q_1, Q_2, and Q_3 pixels for embedding are collected and combined to form bitstream B_1. It is assumed that the patient's record will constitute a sub-bitstream denoted as B_2, which will be embedded into the data. M, LM, B_1, and B_2 are compressed using the JBIG technique to form $M_{comp}, LM_{comp}, B_{1_{comp}}$, and $B_{2_{comp}}$, respectively, and then combined into a single bitstream B. Then, Bitstream B is then embedded into each block, using equation (7) if the embedding procedure uses the location map M, or using equation (8) if it uses the location map LM. The watermarked image is finally produced using equation (6). Finally, The image $I_{src}$is transformed into a watermarked image (W) using the Arnold's Cat Map function $T - k$ times, Fig. 2 illustrates the process, where T denotes the period of the cat map.

2.6.2. Extraction Procedure

Outlined for extraction process is initiated by the Arnold's Cat Map function that applied to the watermarked image W, for a predetermined number of iterations $(k - times)$ to scramble it (Fig. 3). Then, this image is broken up into quad-pixel blocks, with each block becoming a vector $p' = (p'_0, p'_1, p'_2, p'_3)$. The difference in values between these vector $u\tilde{}$ is calculated using Equation (5) to produce a new vector $Q' = (Q'_1, Q'_2, Q'_3)$.Where, vector Q' is classified into two categories, $S_3$and S_4, using Equation (9), where S_3 is contains unchangeable quads, and S_4 is an exception from S_3 used for data embedding. The least significant bits in Q'_1, Q'_2', and Q'_3 of quads S_4 of the categories are collected and combined to form a bitstream B. Bitstream B is partitioned into four segments including $M_{comp}, LM_{comp}, B_{1_{comp}}$,, and $B_{2_{comp}}$.

The JBIG technique is then employed to decompress these segments and generate M, LM, B_1, and B_2. Then, Q_1, Q_2, and Q_3 and $S_1$are determined using the Location Map M, using Equation (17). The original values for v_1, v_2, dan v_3 from S_1 are restored using Q and the Location Map LM through Equation (14).

$$Q_1 = \left\lfloor \frac{Q_1'}{2} \right\rfloor, \quad Q_2 = \left\lfloor \frac{Q_2'}{2} \right\rfloor, \quad Q_3 = \left\lfloor \frac{Q_3'}{2} \right\rfloor \tag{17}$$

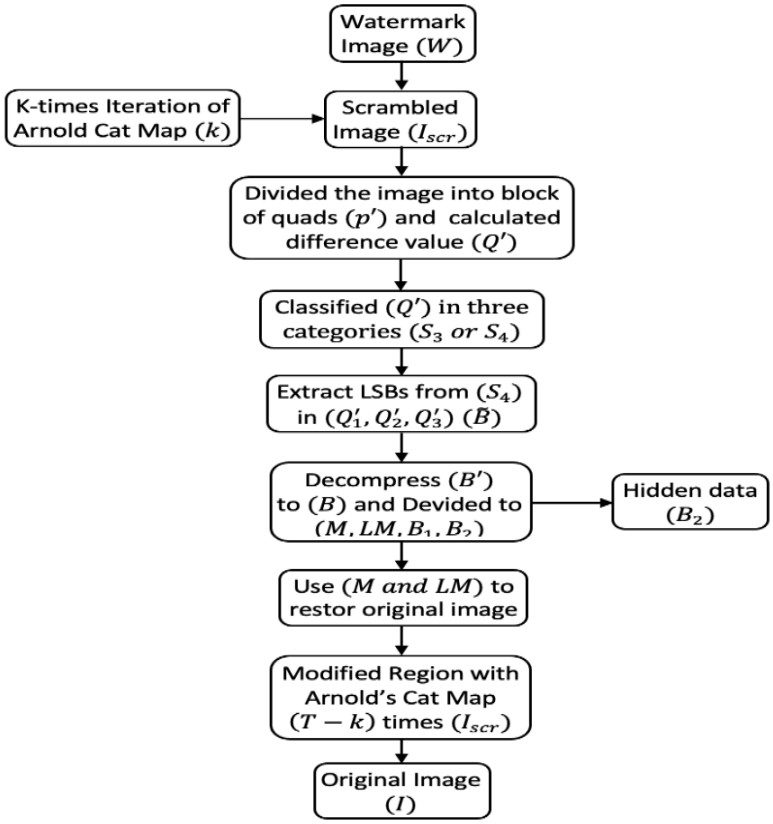

Fig. 3. Extraction procedure of proposed method

The original image will be formed using Equation (6), and the last step was the Arnold's Cat map applied $(T - k)$ times on the modified image I_{src} to obtain the watermarked image, where T is the period of the cat map.

3. Results and Discussion

The evaluation of the proposed method presents the results related to performance, payload, and imperceptibility in this section. Thorough simulations have been conducted using four gray-scale medical image modalities, CT, MRI, Ultrasound, and X-ray, with a size of 200×200 pixels. Fig. 4 depicts four test images. By incorporating the watermark into each and every iteration of the image, the proposed method was evaluated. Two metrics were used to determine how similar the watermarked image and the original image were: PSNR based on Equation (18), and SSIM based on Equation (20).

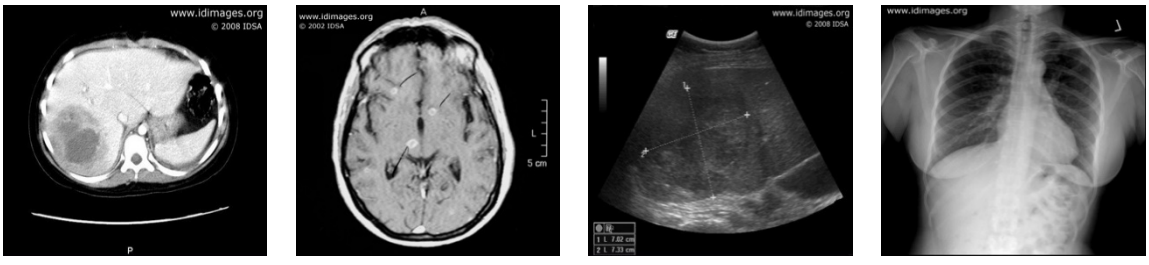

Fig. 4. Four different medical images used for testing [37]

PSNR generates higher values for greater levels of similarity, whereas MSE generates smaller values for better similarity. SSIM is a method used to evaluate how similar two images are, and it aims to improve upon traditional techniques like PSNR that have been found to be unreliable in terms of human perception. The SSIM index is represented by a numerical value that ranges from -1 to 1. A value of 1 indicates that the two images are precisely identical.

$$PSNR(I, I_W) = 10 \log_{10} \frac{255^2}{MSE(I, I_W)} \tag{18}$$

$$MSE(I, I_W) = \frac{1}{m \times n} \sum_{i}^{m-1} \sum_{j}^{n-1} |I(i,j) - I_W(i,j)|^2 \tag{19}$$

$$SSIM(I, I_W) = \frac{(2_{\mu_I \mu_{I_W}} + c_1)(2cov + c_2)}{(\mu_I^2 + \mu_{I_W}^2 + c_1)(\sigma_I^2 + \sigma_{I_W}^2 + c_2)} \tag{20}$$

3.1. Performance Analysis

The tests revealed that the embedding and data extraction processes are efficient and that the image can be reconstructed to its original form. The experimentation showed that by scrambling the image prior to embedding data using the RDH method, the security of data embedding in medical images can be improved. Although Table 1 shows the maximum amount of secret data that we were able to embed using our method, the results indicate that our approach did not produce higher capacity or better visual quality than the previous method described in reference [2].

Table 1. Comparison between previous method [2] and the proposed method

Image	Arham *et al.* [2]		Proposed Method							
			$k-1$		$k-50$		$k-100$		$k-149$	
	Capacity (bpp)	*PSNR (dB)*	*Capacity (bpp)*	*PSNR (dB)*	*Capacity (bpp)*	*PSNR (dB)*	*Capacity (bpp)*	*PSNR (dB)*	*Capacity (bpp)*	*PSNR (dB)*
CT	0.32	39.014	0.30	38.041	0.27	27.745	0.34	26.005	0.31	35.927
MRI	0.62	37.404	0.60	35.960	0.11	31.185	0.27	27.794	0.62	34.407
US	0.42	43.460	0.41	41.021	0.29	33.064	0.36	32.339	0.43	39.546
X-Ray	0.61	42.337	0.60	40.452	0.27	28.121	0.34	26.945	0.61	39.808

3.2. Payload (incorporating capacity)

Based on the results of the tests, the data incorporating capacity in CT, MRI, US, and X-Ray images was found to be good with an average of 0.29 bpp, 0.25 bpp, 0.35 bpp, and 0.35 bpp respectively. The effect of scrambling on the incorporating capacity using the RDH method can be seen from the results obtained. The highest incorporating capacity was found in the initial and final iterations while there was a significant decrease in the middle iterations. This trend can be seen in Fig. 5. In the Arnold's Cat Map algorithm, image scrambling was not as random in the initial and final iterations but was very random in the middle iterations. The highest incorporating capacity was found in MRI images at iteration 149 (0.62 bpp), US images at iteration 149 (0.43 bpp), and X-Ray images at iteration 149 (0.61 bpp). The lowest incorporating capacity was found in MRI images at iteration 40 (0.11 bpp), US images at iteration 40 (0.28 bpp), and X-Ray images at iteration 120 (0.22 bpp). The results for CT images showed that the highest incorporating capacity occurred at iteration 125 with a bpp of 0.36 while the lowest occurred at iteration 138 with a bpp of 0.22. Fig. 4 indicates that scrambling did not have an effect on the incorporating capacity in CT images.

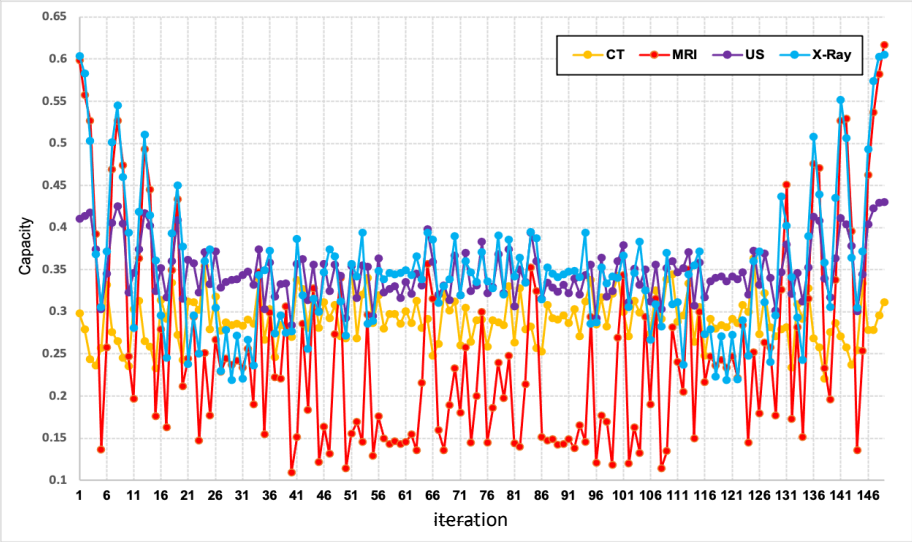

Fig. 5. The proposed method capacity for incorporation was compared to each iteration in the image

3.3. Imperceptibility

According to the test results, the quality of the images after the embedding procedure satisfies the requirements. The average quality of the images in CT, MRI, US, and X-Ray images after the embedding procedure was determined to be 27.75 dB, 29.89 dB, 33.15 dB, and 28.08 dB based on PSNR, and 0.7599, 0.8731, 0.8220, and 0.7268 based on SSIM. Although the randomization process before the embedding data using the RDH method affects the image quality, the results showed that the image quality still decreased after the embedding. The best image quality in CT, MRI, US, and X-Ray images was achieved in the first iteration, with 38.04 dB, 35.96 dB, 41.02 dB, and 40.45 dB based on PSNR and 0.9923, 0.9860, 0.9900, and 0.9864 based on SSIM, respectively. On the other hand, the worst image quality was recorded in iterations 100, 54, 26, and 41, with 26.01 dB, 27.51 dB, 32.27 dB, and 25.63 dB based on PSNR and 0.6811, 0.8121, 0.7844, and 0.6132 based on SSIM, respectively. After embedding data using the RDH method, the tests revealed that the randomization process affects image quality. At the start and end of the iterations, the image quality is relatively good, but significantly decreases in the middle iterations, as shown in Fig. 6 and Fig. 7 . In the Arnold's Cat Map algorithm, the randomization process of the images is not very random at the start and end of the iterations, but is highly random in the middle iteration.

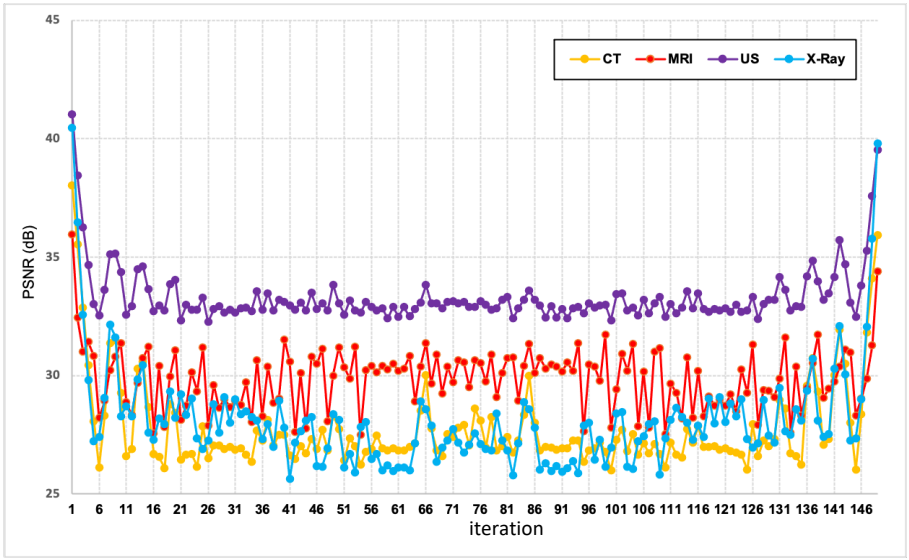

Fig. 6. The proposed method visual quality was compared to each iteration in the image in terms of PSNR

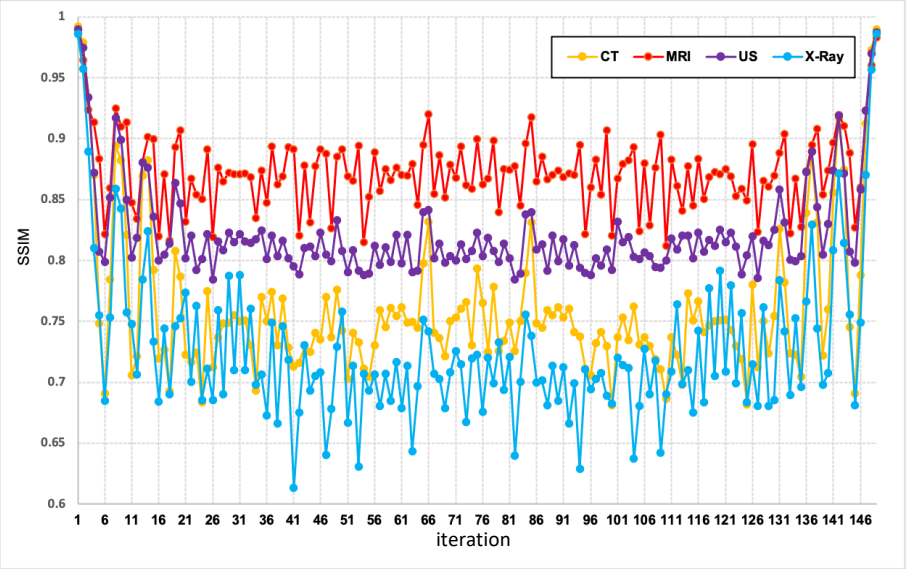

Fig. 7. The proposed method visual quality was compared to each iteration in the image in terms of SSIM

4. Conclusion

Recently, there have been recent advancements in data hiding techniques for medical images, with RDH being a suitable method. However, security remains a concern with RDH methods, as unauthorized individuals can easily access and modify the embedded data if they are aware of the technique used. In the past, one solution to this issue was to encrypt the confidential data before embedding it to enhance the security of the RDH approach. This study proposes a method to further enhance the security of the RDH method in medical images by incorporating the Arnold's Cat Map algorithm and the Chaotic Map into the Difference Expansion (DE) method. The proposed method can securely hide data in medical images and restore the original image after extraction. Although our method did not improve the capacity or visual quality compared to the approach mentioned in reference [2], it is still easy to implement and straightforward. The image quality after data hiding is acceptable, as demonstrated by the high PSNR and SSIM values obtained. If the proposed method is applied with encrypted data, it would enhance the security level of the RDH methods.

Declarations

Author contribution. Aulia Arham: designing methodology, coding, experiment, writing, analysing funding; and Novia Lestari: reviewing, designing methodology, editing.
Funding statement. This research was funded by by the Department of Information System, State Islamic University Imam Bonjol, Padang, Indonesia.
Conflict of interest. The authors declare no conflict of interest.
Additional information. No additional information is available for this paper.

References

[1] A. Arham and O. Secio Riza, "Reversible Data Hiding Using Hybrid Method of Difference Expansion on Medical Image," *J. Ilm. Tek. Elektro Komput. dan Inform.*, vol. 6, no. 2, p. 11, Jan. 2021, doi: 10.26555/jiteki.v6i2.16965.

[2] A. Arham, H. A. Nugroho, and T. B. Adji, "Multiple Layer Data Hiding Scheme Based on Difference Expansion of Quad," *Signal Processing*, vol. 137, pp. 52–62, 2017, doi: 10.1016/j.sigpro.2017.02.001.

[3] A. Arham, H. A. Nugroho, and T. B. Adji, "Combination schemes Reversible Data Hiding for medical images," in *Science and Technology-Computer (ICST), International Conference on*, 2016, pp. 44–49, doi: 10.1109/ICSTC.2016.7877345.

[4] W. Wang, "A reversible data hiding algorithm based on bidirectional difference expansion," *Multimed. Tools Appl.*, vol. 79, no. 9, pp. 5965–5988, 2020, doi: 10.1007/s11042-019-08255-z.

[5] M. Nazari and M. Mehrabian, "A novel chaotic IWT-LSB blind watermarking approach with flexible capacity for secure transmission of authenticated medical images," *Multimed. Tools Appl.*, vol. 80, no. 7, pp. 10615–10655, 2021, doi: 10.1007/s11042-020-10032-2.

[6] K. Balasamy and S. Suganyadevi, "A fuzzy based ROI selection for encryption and watermarking in medical image using DWT and SVD," *Multimed. Tools Appl.*, vol. 80, no. 5, pp. 7167–7186, 2021, doi: 10.1007/s11042-020-09981-5.

[7] E. E.-D. Hemdan, "An efficient and robust watermarking approach based on single value decompression, multi-level DWT, and wavelet fusion with scrambled medical images," *Multimed. Tools Appl.*, vol. 80, no. 2, pp. 1749–1777, 2021, doi: 10.1007/s11042-020-09769-7.

[8] A. Al-Haj and H. Abdel-Nabi, "An efficient watermarking algorithm for medical images," *Multimed. Tools Appl.*, vol. 80, no. 17, pp. 26021–26047, 2021, doi: 10.1007/s11042-021-10801-7.

[9] R. Thanki and S. Borra, "Fragile watermarking for copyright authentication and tamper detection of medical images using compressive sensing (CS) based encryption and contourlet domain processing," *Multimed. Tools Appl.*, vol. 78, no. 10, pp. 13905–13924, 2019, doi: 10.1007/s11042-018-6746-2.

[10] R. Thanki and A. Kothari, "Multi-level security of medical images based on encryption and watermarking for telemedicine applications," *Multimed. Tools Appl.*, vol. 80, no. 3, pp. 4307–4325, 2021, doi: 10.1007/s11042-020-09941-z.

[11] A. K. Singh, "Robust and distortion control dual watermarking in LWT domain using DCT and error correction code for color medical image," *Multimed. Tools Appl.*, vol. 78, no. 21, pp. 30523–30533, 2019, doi: 10.1007/s11042-018-7115-x.

[12] F. Sabbane and H. Tairi, "Medical image watermarking technique based on polynomial decomposition," *Multimed. Tools Appl.*, vol. 78, no. 23, pp. 34129–34155, 2019, doi: 10.1007/s11042-019-08134-7.

[13] T.-C. Lu and T. N. Vo, "Introduction of Reversible Data Hiding Schemes," in *International Conference on Security with Intelligent Computing and Big-data Services*, 2019, pp. 170–183, doi: 10.1007/978-3-030-46828-6_15.

[14] G. Gao, S. Tong, Z. Xia, B. Wu, L. Xu, and Z. Zhao, "Reversible data hiding with automatic contrast enhancement for medical images," *Signal Processing*, vol. 178, p. 107817, 2021, doi: 10.1016/j.sigpro.2020.107817.

[15] S. Weng, W. Tan, B. Ou, and J.-S. Pan, "Reversible data hiding method for multi-histogram point selection based on improved crisscross optimization algorithm," *Inf. Sci. (Ny).*, vol. 549, pp. 13–33, 2021, doi: 10.1016/j.ins.2020.10.063.

[16] P. Maniriho, L. J. Mahoro, Z. Bizimana, E. Niyigaba, and T. Ahmad, "Reversible difference expansion multi-layer data hiding technique for medical images," *Int. J. Adv. Intell. Informatics*, vol. 7, no. 1, pp. 1–11, 2021, doi: 10.26555/ijain.v7i1.483.

[17] Z. Syahlan and T. Ahmad, "Reversible data hiding method by extending reduced difference expansion," *Int. J. Adv. Intell. Informatics*, vol. 5, no. 2, pp. 101–112, 2019, doi: 10.26555/ijain.v5i2.351.

[18] J. Tian, "Reversible data embedding using a difference expansion," *IEEE Trans. Circuits Syst. Video Technol.*, vol. 13, no. 8, pp. 890–896, 2003, doi: 10.1109/TCSVT.2003.815962.

[19] T.-S. Nguyen, V.-T. Huynh, and P.-H. Vo, "A Novel Reversible Data Hiding Algorithm Based on Enhanced Reduced Difference Expansion," *Symmetry (Basel).*, vol. 14, no. 8, p. 1726, 2022, doi: 10.3390/sym14081726.

[20] Y. Samudra and T. Ahmad, "Improved prediction error expansion and mirroring embedded samples for enhancing reversible audio data hiding," *Heliyon*, vol. 7, no. 11, p. e08381, 2021, doi: 10.1016/j.heliyon.2021.e08381.

[21] A. J. Ilham and T. Ahmad, "Reversible Data Hiding Scheme based on General Difference Expansion Cluster," *Int. J. Adv. Soft Comput. Appl.*, vol. 12, no. 3, pp. 12-24, 2020. [Online]. Available at: http://188.247.81.52/.

[22] C.-F. Lee, J.-J. Shen, and C.-Y. Wu, "Hiding Scheme based on Improved Reduced Difference Expansion in Multi-block Shape," in *Advances in Intelligent Information Hiding and Multimedia Signal Processing:*

Proceeding of the IIH-MSP 2021 & FITAT 2021, Kaohsiung, Taiwan, Volume 2, Springer, 2022, pp. 297–310, doi: 10.1007/978-981-19-1053-1_27.

[23] T. Ahmad, H. I. Dewangkoro, W. Wibisono, and R. M. Ijtihadie, "Protecting Data by Improving the Performance of Controlling Expansion Method," in *Advances in Cyber Security: Second International Conference, ACeS 2020, Penang, Malaysia, December 8-9, 2020, Revised Selected Papers 2*, 2021, pp. 577–587, doi: 10.1007/978-981-33-6835-4_38.

[24] N. J. de La Croix, C. C. Islamy, and T. Ahmad, "Reversible Data Hiding using Pixel-Value-Ordering and Difference Expansion in Digital Images," in *2022 IEEE International Conference on Communication, Networks and Satellite (COMNETSAT)*, 2022, pp. 33–38, doi: 10.1109/COMNETSAT56033.2022.9994516.

[25] A. Mehbodniya *et al.*, "Multilayer Reversible Data Hiding Based on the Difference Expansion Method Using Multilevel Thresholding of Host Images Based on the Slime Mould Algorithm," *Processes*, vol. 10, no. 5, p. 858, 2022, doi: 10.3390/pr10050858.

[26] P. Maniriho and T. Ahmad, "Information hiding scheme for digital images using difference expansion and modulus function," *J. King Saud Univ. Inf. Sci.*, vol. 31, no. 3, pp. 335–347, 2019, doi: 10.1016/j.jksuci.2018.01.011.

[27] P. Maniriho and T. Ahmad, "Enhancing the Capability of Data Hiding Method Based on Reduced Difference Expansion.," *Eng. Lett.*, vol. 26, no. 1, p. 11, 2018. [Online]. Available at: https://www.researchgate.net/profile/Pascal-.

[28] C.-F. Lee, J. J. Shen, and Y. H. Lai, "Data hiding using multi-pixel difference expansion," in *2018 3rd International Conference on Computer and Communication Systems (ICCCS)*, 2018, pp. 56–60, doi: 10.1109/CCOMS.2018.8463244.

[29] P. C. Mandal, I. Mukherjee, and B. N. Chatterji, "High capacity reversible and secured data hiding in images using interpolation and difference expansion technique," *Multimed. Tools Appl.*, vol. 80, no. 3, pp. 3623–3644, 2021, doi: 10.1007/s11042-020-09341-3.

[30] X. Wu, T. Qiao, M. Xu, and N. Zheng, "Secure reversible data hiding in encrypted images based on adaptive prediction-error labeling," *Signal Processing*, vol. 188, p. 108200, 2021, doi: 10.1016/j.sigpro.2021.108200.

[31] A. Meenpal and S. Majumder, "Image content based secure reversible data hiding scheme using block scrambling and integer wavelet transform," *Sādhanā*, vol. 47, no. 2, p. 54, 2022, doi: 10.1007/s12046-022-01828-z.

[32] M. Fadhil *et al.*, "Secure Reversible Data Hiding in the Medical Image using Histogram Shifting and RC4 Encryption," in *2019 International Seminar on Application for Technology of Information and Communication (iSemantic)*, 2019, pp. 1–6, doi: 10.1109/ISEMANTIC.2019.8884306.

[33] S. Kukreja and G. Kasana, "A secure reversible data hiding scheme for digital images using random grid visual secret sharing," in *2019 Amity International Conference on Artificial Intelligence (AICAI)*, 2019, pp. 864–869, doi: 10.1109/AICAI.2019.8701360.

[34] M. Nasir *et al.*, "Secure Reversible Data Hiding in Images Based on Linear Prediction and Bit-Plane Slicing," *Mathematics*, vol. 10, no. 18, p. 3311, 2022, doi: 10.3390/math10183311.

[35] S. Kamil Khudhair, M. Sahu, R. KR, and A. K. Sahu, "Secure Reversible Data Hiding Using Block-Wise Histogram Shifting," *Electronics*, vol. 12, no. 5, p. 1222, 2023, doi: 10.3390/electronics12051222.

[36] A. K. Sahu, "A logistic map based blind and fragile watermarking for tamper detection and localization in images," *J. Ambient Intell. Humaniz. Comput.*, vol.13, no. 8, pp. 3869-3881, 2021, doi: 10.1007/s12652-021-03365-9.

[37] "Partners Infectious Disesase Images, Emicrobes Digital Library.". [Online]. Available at: https://cfar.globalhealth.harvard.edu/pages/partners-infectious-disease-images.